THE JOURNAL OF BIOLOGICAL CHEMISTRY VOL. 288, NO. 10, pp. 7294–7304, March 8, 2013

Identification and Analysis of a Novel Dimerization Domain Shared by Various Members of c-Jun N-terminal Kinase (JNK) Scaffold Proteins*[S]

Received for publication, September 23, 2012, and in revised form, December 31, 2012 Published, JBC Papers in Press, January 22, 2013, DOI 10.1074/jbc.M112.422055

Ksenya Cohen-Katsenelson[‡1], Tanya Wasserman[‡1], Ilona Darlyuk-Saadon[‡1], Alona Rabner[§], Fabian Glaser[§], and Ami Aronheim[‡2]

From the [‡]Department of Molecular Genetics, The Rappaport Faculty of Medicine and Research Institute, Technion-Israel Institute of Technology, Haifa 31096, Israel and the [§]Bioinformatics Knowledge Unit, The Lorry I. Lokey Interdisciplinary Center for Life Sciences and Engineering, Technion, Haifa 32000, Israel

Background: WDR62 is a JNK scaffold protein.
Results: We identified at the WDR62 C terminus a loop-helix domain that is responsible for its homodimerization and association with another JNK scaffold protein, MAPKBP1. WDR62 dimerization is required for JNK and MKK7β1 recruitment.
Conclusion: WDR62 dimerization is required for its scaffolding function.
Significance: Scaffold protein association offers another layer of complexity for the fine tuning of signaling pathways.

Mitogen-activated protein kinases (MAPKs) form a kinase tier module in which MAPK, MAP2K, and MAP3K are held by scaffold proteins. The scaffold proteins serve as a protein platform for selective and spatial kinase activation. The precise mechanism by which the scaffold proteins function has not yet been fully explained. WDR62 is a novel scaffold protein of the c-Jun N-terminal kinase (JNK) pathway. Recessive mutations within WDR62 result in severe cerebral cortical malformations. One of the WDR62 mutant proteins found in a patient with microcephaly encodes a C-terminal truncated protein that fails to associate efficiently with JNK and MKK7β1. The present article shows that the WDR62 C-terminal region harbors a novel dimerization domain composed of a putative loop-helix domain that is necessary and sufficient for WDR62 dimerization and is critical for its scaffolding function. The loop-helix domain is highly conserved between orthologues and is also shared by the JNK scaffold protein, JNKBP1/MAPKBP1. Based on the high sequence conservation of the loop-helix domain, our article shows that MAPKBP1 homodimerizes and heterodimerizes with WDR62. Endogenous WDR62 and MAPKBP1 co-localize to stress granules following arsenite treatment, but not during mitosis. This study proposes another layer of complexity, in which coordinated activation of signaling pathways is mediated by the association between the different JNK scaffold proteins depending on their biological function.

Mitogen-activated protein kinase (MAPK) signaling pathways consist of a large family of protein kinases that enable cells to respond to a range of extracellular signals. The MAPKs form a cellular network that translates and transfers extracellular cues into complex cytoplasmic and nuclear processes, resulting in an appropriate cellular response. The MAPK signaling pathway is composed of a three-main-tiered signaling module, consisting of MAP3Ks, MAP2Ks, and MAPKs (1). Three groups of mammalian MAPKs have been studied most extensively, including extracellular signal-regulated kinases (ERKs), stress-activated protein kinases known as c-Jun N-terminal kinases (JNKs), and p38 (2, 3). Numerous studies have shown that the various MAPK modules regulate distinctly different cellular responses in a cell type- and/or context-specific manner. With regard to the JNK pathway, 14 different MAP3Ks have been described as activating two MAP2K kinases that activate three distinct JNK isoforms (representing a total of 10 splice variants) (4, 5). The main challenge in deciphering the network of various signaling pathways and their unique cellular response is to reveal the molecular mechanism involved in signal specificity (6). Recently, the importance of scaffold proteins has been shown to be responsible for the assembly of a discrete set of signaling proteins into a functional protein complex. Scaffold proteins generally do not have any catalytic activity and are defined by their ability to coordinate the association of two or more proteins of the MAPK tier. The proximity of the interacting signaling proteins in one complex increases the effectiveness of the signaling pathway by simply tethering the proteins and correctly orienting the substrate with its enzyme. This causes signal amplification and restriction of the proteins to specific pathways. Scaffold proteins are composed of numerous modular protein-protein interaction domains (2). Multiple JNK scaffold proteins have been described, including the JNK-interacting proteins (JIP1–4),[3] plenty of SH3s (POSH), β-arrestin,

* This work was supported by the Israeli Science Foundation Grant 573/11 (to A. A.).
[S] This article contains supplemental Figs. 1–6.
[1] These authors contributed equally to this work.
[2] To whom correspondence should be addressed: Dept. of Molecular Genetics, The Rappaport Family Institute for Research in the Medical Sciences, Technion-Israel Institute of Technology, 1 Efron St., Bat-Galim, Haifa 31096, Israel. Tel.: 972-4-8295454; Fax: 972-4-8295225; E-mail: aronheim@tx.technion.ac.il.

[3] The abbreviations used are: JIP, JNK-interacting protein; BLZ, basic leucine zipper; DLK, dual leucine zipper-bearing kinase; JNKBP1/MAPKBP1, JNK/MAPK-binding protein 1; LCK, lymphocyte-specific protein tyrosine kinase; MLK, mixed lineage kinase; POSH, plenty of SH3s; WCE, whole cell extract; WDR62, WD40 repeat domain 62.

IκB kinase complex-associated protein (IKAP) (7), JNK-binding protein 1 (JNKBP1/MAPKBP1) (8, 9), and the recently described WDR62 (10, 11). The JNK scaffold proteins are extremely diverse proteins that share low sequence conservation. WDR62 was identified in a modified protein-protein interaction screen in yeast based on its ability to associate with JNK (10). Interestingly, WDR62 was found to be mutated in patients with microcephaly (12–17). A relatively large number of WDR62 mutations, including missense mutations and premature translation terminations, have been identified in patients, all of which cause a similar severe phenotype. It has been hypothesized that WDR62 plays a developmental role early in embryogenesis and that its functional impairment results in the development of microcephaly and pachygyria (18). WDR62 is localized to the centrosome during mitosis (13) and, following oxidative stress is found in stress granules (10). The role of WDR62 during mitosis was studied recently using its depletion by siRNA. WDR62 was found to regulate spindle orientation, centrosome integrity, and mitotic progression (19). WDR62 does not share obvious sequence homology with any of the known proteins in the data bank and possesses no enzymatic activity (10). Structure function analysis revealed that WDR62 can associate with at least two components of the JNK signaling pathway including JNK and MKK4/7. The association occurs via two distinct docking domains that are located at amino acids 1294–1301 and 1212–1284, respectively (11). The WDR62 N-terminal domain contains 12 repeats of a WD40 domain, to which no functional activity has yet been assigned (10). In the present article, we describe the identification of a novel dimerization domain within WDR62 located at its C-terminal domain downstream from MKK7β1 and JNK association domains. WDR62, which lacks the dimerization domain, fails to associate efficiently with either JNK or MKK7β1 (11). WDR62 dimerization is critical for its scaffolding function with JNK and MKK7β1. This novel domain is highly conserved among WDR62 orthologues and is also shared by JNKBP1/MAPKBP1 JNK scaffold protein (8). The dimerization domain enables MAPKBP1 to both homodimerize and heterodimerize with WDR62.

EXPERIMENTAL PROCEDURES

Materials—Arsenite (Fluka, 71287) was dissolved in PBS to generate 50 mM stock solution. Collagen (Roche Applied Science, 11179179001) was dissolved in 0.2% acetic acid to generate 2 mg/ml stock solution.

Antibodies—The following antibodies were used: anti-Myc monoclonal (9E10), anti-HA monoclonal (12CA5), anti-GST rabbit polyclonal (produced in our own laboratory), anti-MAPKBP1 polyclonal (D-15) (Santa Cruz Biotechnology, sc-164964), anti-WDR62 (3G8) monoclonal (Sigma-Aldrich, W3269), anti-WDR62 (JBP5) polyclonal (produced in our own laboratory, as described previously (10)), anti-DCP1A monoclonal (Abnova, H00055802-M06). Fluorochrome-tagged secondary antibodies for immunofluorescence assays were obtained from Jackson ImmunoResearch Laboratories.

Plasmids—The mammalian expression plasmids pCAN and pcDNA 3XHA were used to express all Myc-tagged and HA-tagged human WDR62 deletion mutants, respectively. Human WDR62 fragments fused to GST were designed in the mammalian expression vector pcDNA3-GST-V3, in which the WDR62 fragments were generated by PCR and inserted by a HindIII-XhoI restriction, as described previously (11). All deletion constructs were designated according to their amino acid position within the human CS5 isoform. The letters N and C represent amino acids 1 and 1523, respectively. The first and last three amino acids of all constructs used in this study are shown in Table 1. All corresponding oligonucleotides designed for the PCR can be provided upon request.

TABLE 1
First and last three amino acids of all constructs used in this study

WDR62 construct	Amino acid start	Amino acid end
Full-length	MAA	RGH
N-1401	MAA	EPW
N-1284	MAA	EPA
1018-C	RFA	RGH
NG 26-1	RFA	EPW
NG 26-1-α1α2	RFA	DLQ
NG 26-1-α3	RFA-EPW	TSV-RGH
1018–1284	RFA	EPA
1212-C	PST	RGH
1285-C	LRS	RGH
1402-C	VPV	RGH
Human c-Jun (248–332)	ESQ	QTF
MAPKBP1-C	HLV	RKL

HA-tagged human JNK2 was expressed using the pSRα mammalian expression plasmid. The mammalian expression plasmid pEBG was used to express GST-tagged human JNK2 and MKK7β1 (20). MAPKBP1 expression plasmid was kindly provided by Drs. Katsuji Yoshioka and Michihiko Ito (8). The C-terminal fragment was generated by PCR and cloned into HA- and Myc-tagged expression plasmids as described above.

Cell Culture and Transient Transfection—HEK-293T cells were maintained in Dulbecco's modified Eagle's medium (DMEM) containing 10% FCS, 100 units/ml penicillin, and 0.1 μg/ml streptomycin, and grown at 37 °C with 5% CO_2. HEK-293T cells were transfected with the appropriate combination of expression plasmids using the calcium phosphate (Ca_2PO_4) method (11). The total amount of plasmid DNA was adjusted to 10–12 μg in a total volume of 1000 μl. Cells were replaced with fresh medium 4–5 h after transfection and harvested 24 h thereafter.

Immunoprecipitations—Cells were lysed in a whole cell extraction buffer (WCE, 25 mM HEPES, pH 7.7, 0.3 M NaCl, 1.5 mM $MgCl_2$, 0.2 mM EDTA, 0.1% Triton X-100, 0.5 mM DTT, 20 mM β-glycerolphosphate, 0.1 mM Na_2VO_4, 100 μg/ml PMSF, protease inhibitor mixture 1:100 (Sigma Aldrich, P8340)). The lysates were centrifuged at maximal speed for 10 min to pellet cellular debris, and the supernatant was used as the protein extract. Protein extract (400–600 μg in WCE buffer) was precleared with nonrelevant antibodies. The lysate was then incubated overnight with the indicated primary antibodies at 4 °C. Protein A-Sepharose beads (Sigma-Aldrich, P3391) were then added to the lysate and incubated for 1 h. Samples were washed four times with WCE extraction buffer. The precipitated proteins were eluted using SDS-PAGE sample buffer, boiled (except those complexes containing full-length WDR62 protein), and then processed for Western blot analysis.

GST Pulldown Assay—Glutathione-agarose beads (Sigma-Aldrich, G4510) were preblocked with 5% BSA and then incu-

bated with 400–600 μg of the protein extract (in WCE buffer). Following four washes with the WCE extraction buffer, the precipitated proteins were eluted using freshly made glutathione elution buffer (50 mM Tris, pH 8.0, 20 mM L-glutathione (Sigma-Aldrich, G4251), 1 mM DTT, 1 mM PMSF). The samples (except those containing full-length WDR62 protein) were boiled and then processed for Western blot analysis.

Western Blot Analysis—Protein samples were separated by 10% SDS-PAGE, followed by transfer to nitrocellulose membrane. Blots were blocked in 5% dry milk in PBS and washed in PBS. Proteins were detected using the corresponding HRP-conjugated secondary antibodies obtained from Sigma-Aldrich (anti-rabbit A0545, anti-mouse A0168) and Jackson (anti-mouse light chain 115-035-174, anti-rabbit light chain 211-032-171).

Immunofluorescence—HEK-293T cells were grown on glass coverslips coated with collagen. Following transfection or cellular stimulation, cells were fixed with 4% formaldehyde for 10 min. After being washed with PBS, the cells were permeabilized with 0.1% Triton X-100 for 5 min and incubated in a blocking solution of 5% FCS in PBS for 30 min. The cells were then incubated with the appropriate primary antibodies mixture for 1 h in PBS containing 1% FCS. The cells were washed three times with PBS and incubated with a secondary fluorescent antibodies mix for 1 h in PBS containing 2% BSA, 2% FCS, and 0.1% Tween 20. The cells were washed twice with PBS and processed for nuclear staining using DAPI (Sigma-Aldrich, D9542) at a final concentration of 1 μg/μl in PBS. The stained cells were then washed twice with PBS and mounted in Fluoromount-G (Southern Biotechnology, 0100-01).

Confocal Microscopy—Fluorescence microscopy was performed using a Zeiss LSM 510 Meta inverted confocal microscope equipped with a ×63/1.4 NA (numerical aperture) oil objective, multiline argon laser (488, 514 nm), DPSS (diode-pumped solid-state) laser (561 nm), and a UV diode laser (405 nm). Each image was acquired from a single 1-μm-thick Z-stack using 510 LSM software (Zeiss).

Bioinformatics Analysis—A sequence of the last (C terminus) 520 amino acids was used against Uniprot by the phmmer application of the HMMER server to recover the initial list of 61 WDR62 sequence homologues (21). Removing fragmented sequences and realigning them produced a PRANK alignment (22) that was used to obtain additional homologues with the hmmsearch application of the HMMER server (23). This resulted in a larger redundant list of 94 more distant homologues (up to 80% identity). To filter out redundant sequences a phylogenetic tree was built by FastTree (23), which revealed two different orthologues. After redundant, partial, and fragmented sequences had been removed a final list of 30 sequences remained, for which the last 200 amino acids of each sequence were used to create a new final alignment by SATe (24). This alignment was used by ConSurf (25, 26) to calculate the evolutionary conservation scores and by GeneSilico server (27) to estimate secondary structure. WebLogo was performed as described (28).

Statistical Analysis—Statistical analysis was performed using Student's unpaired *t* test with one-tailed distribution.

RESULTS

Full-length WDR62 Forms Homodimers—Protein scaffolds typically dimerize to form a dual scaffolding platform for association with multiple proteins (29). WDR62 is a recently identified JNK scaffold protein that has no obvious sequence homology to known proteins (10). Importantly, WDR62 does not harbor any known protein dimerization motif. To investigate whether WDR62 forms dimers, we fused Myc-tagged WDR62 CS5 cDNA to GST (Myc-WDR62-GST) and tested its ability to pull down Myc-tagged WDR62 using a GST pulldown assay in HEK-293T cells (Fig. 1*A*). The tagged proteins can be easily distinguished by the slower migration of the Myc-WDR62-GST protein on SDS-PAGE (Fig. 1*B*, *middle panel*, *lane 4*). The GST pulldown assay revealed that Myc-tagged WDR62 is efficiently co-precipitated with Myc-WDR62-GST, which demonstrates the ability of WDR62 to form homodimers (Fig. 1*B*, *top panel*, *lane 4*). No protein is observed in the GST-only pulldown (Fig. 1*B*, *top panel*, *lanes 1–3*).

Mapping WDR62 Dimerization Domain—Because the WDR62 sequence does not display any homology with a known dimerization motif, we sought to map the domain responsible for WDR62 homodimerization. First, we deleted the increasing C-terminal portions from the Myc-WDR62 construct to create two constructs, Myc-N-1401 and Myc-N-1284. The former construct represents a deletion found in a human patient, NG 26-1 (12), and is referred to hereafter as Myc-NG 26-1. Both C-terminal deleted fragments were unable to dimerize with Myc-WDR62-C-GST (Fig. 1*B*, *top panel*, *lanes 5* and *6*). These results show that the domain necessary for dimerization lies within the 122-amino acid region at the C terminus.

The C-terminal region that was found to be necessary for WDR62 dimerization can either self-associate or form protein-protein interaction with an internal domain. To differentiate between these two possibilities, we designed a GST-tagged construct encoding a shorter C-terminal fragment composed of the last 122 amino acids (1402-C-GST) and tested its ability to interact with Myc-1402-C, Myc-1285-C, Myc-1018–1284, and Myc-1018-C (Fig. 2*A*). The 1402-C-GST fragment was associated with all of the fragments that included the last 122 amino acids from the C-terminal domain intact (Fig. 2*B*, *top panel*, *lanes 5*, *7*, and *8*), but not with the fragment lacking the C terminus (Myc-1018–1284, Fig. 2*B*, *top panel*, *lane 6*). Collectively, the WDR62 fragment containing the last 122 amino acids is both necessary and sufficient to form dimers.

To examine whether the endogenous WDR62 protein is able to form dimers, HEK-293T cells were transfected with either Myc-1018-C or the corresponding fragment lacking the putative dimerization domain, Myc-NG 26-1 (1018–1401). We used the WDR62 monoclonal antibodies (anti-3G8, Sigma-Aldrich), directed against the WD40 domain, to immunoprecipitate endogenous WDR62 to test whether the transfected WDR62 fragment could be co-precipitated (Fig. 2*C*). Whereas the wild-type Myc-1018-C was efficiently co-precipitated by the 3G8 antibody (Fig. 2*C*, *lane 5*), no co-precipitation was observed in cell lysate derived from Myc-NG 26-1-transfected cells (Fig. 2*C*, *lane 6*). Importantly, endogenous WDR62 protein

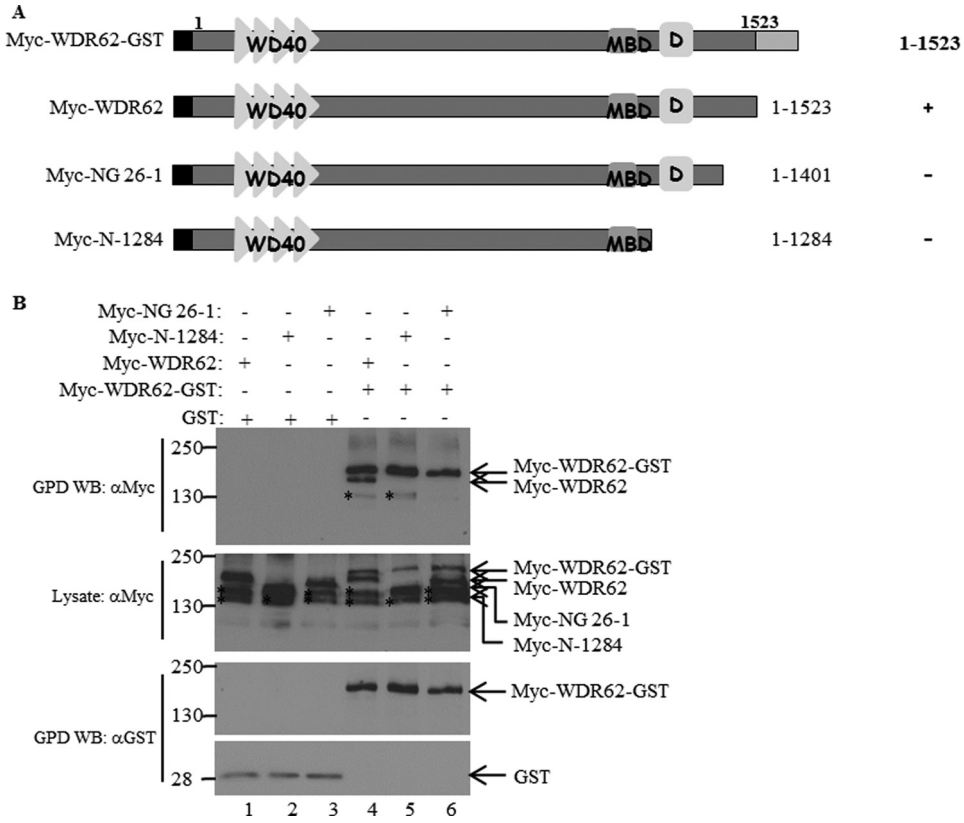

FIGURE 1. **The C-terminal domain is necessary for dimerization of the full-length WDR62.** *A*, schematic represents the WDR62 deletion constructs used in the experiments. The *light gray rectangle* represents the position of the GST tag. The *black square* represents the position of the Myc epitope tag. The WD40 domain (*WD40*), MKK7 binding domain (*MBD*), and the JNK docking domain (*D*) are indicated. Summary of the binding of the various WDR62 fragments to WDR62-GST is indicated by +/−. *B*, HEK-293T cells were transfected with the indicated plasmids. GST-containing complexes were isolated from cell lysates with glutathione-agarose beads, washed extensively, and eluted with reduced glutathione (*GPD*). The protein complexes were subjected to Western blotting with either anti-Myc (*top panel*) or anti-GST (*bottom panel*) antibodies. The expression level of transfected WDR62 fragments was determined by blotting the total cell lysate with an anti-Myc antibody (*middle panel*). The migration of the relevant proteins is indicated by *arrows*. The *asterisks* (*) indicate nonspecific bands on the *left corner* of the corresponding *lane*.

is readily observed in all anti-3G8 but not with anti-HA immunoprecipitates (Fig. 2*C*, *lanes 4–6*).

WDR62 Homodimerization Is Necessary for Its Scaffolding Function—Next we sought to investigate the functional relevance of WDR62 dimerization. To this end, we compared the ability of a WDR62 fragment (Myc-1018-C) and the dimerization mutant protein lacking the last 122 amino acids (amino acids 1018–1401, Myc-NG 26-1) to associate with HA-JNK2 (Fig. 3*A*). Of note, the NG 26-1 mutant, which lacks the putative dimerization domain, contains the JNK2 and MKK7 binding domains. Interestingly, NG 26-1 mutant protein displayed an 8-fold lower association with JNK2, compared with the wild-type WDR62 fragment containing the entire C-terminal region (Fig. 3, *B*, compare *lanes 2* and *3*, and *C*). Furthermore, the NG 26-1 mutant also failed to associate efficiently with MKK7β1 (Fig. 3*D*). The NG 26-1 fragment, which lacks the dimerization domain, displayed 3-fold reduced recruitment of MKK7, compared with the wild-type WDR62 fragment (Fig. 3*E*). To reveal whether WDR62 dimerization *per se* enhances the association with JNK2 and MKK7β1, we fused both Myc- and HA-tagged versions of NG 26-1 WDR62 mutant protein to the basic leucine zipper domain derived from c-Jun, a member of the AP-1 family of transcription factors (BLZ, Fig. 3*A*) (30, 31). Indeed, the NG 26-1 mutant fused to the c-Jun basic leucine zipper domain (NG 26-1-Jun) was able to form dimers, as demonstrated by precipitation of the HA-tagged fragment with anti-Myc antibody only in the presence of the corresponding Myc-tagged NG 26-1-Jun protein (supplemental Fig. 1, *lane 3*). Importantly, the reconstitution of the NG 26-1 ability to form dimers, via the c-Jun leucine zipper domain, fully recapitulated its ability to associate with HA-JNK2 (Fig. 3, *B*, *lane 4*, and *C*), but not the binding to MKK7β1 (Fig. 3, *D*, *lane 6*, and *E*). These data suggest that WDR62 dimerization is necessary and sufficient for the strong association with JNK2 but not sufficient to fully recapitulate the association with MKK7β1.

The WDR62 Homodimerization Domain Is Composed of Three Putative α-Helices—The WDR62 C-terminal domain displays no sequence homology with any known dimerization motif. To further define the structural requirements responsible for the WDR62 dimerization domain, we used bioinformatics analysis of the last 200 amino acids. Based on sequence conservation, secondary structure prediction, and structural analysis, we were able to suggest the possible existence of three putative α-helices in the C-terminal region of WDR62 (Fig. 4*A*). The last α-helix (the closest to the C terminus) displayed the highest evolutionary conservation among the WDR62 orthologues (Fig. 4*A*). To examine the role of the third α-helix, we designed a WDR62 protein in which the first two α-helices were deleted while preserving the last 49 amino acids, which contained a putative loop motif followed by the third α-helix

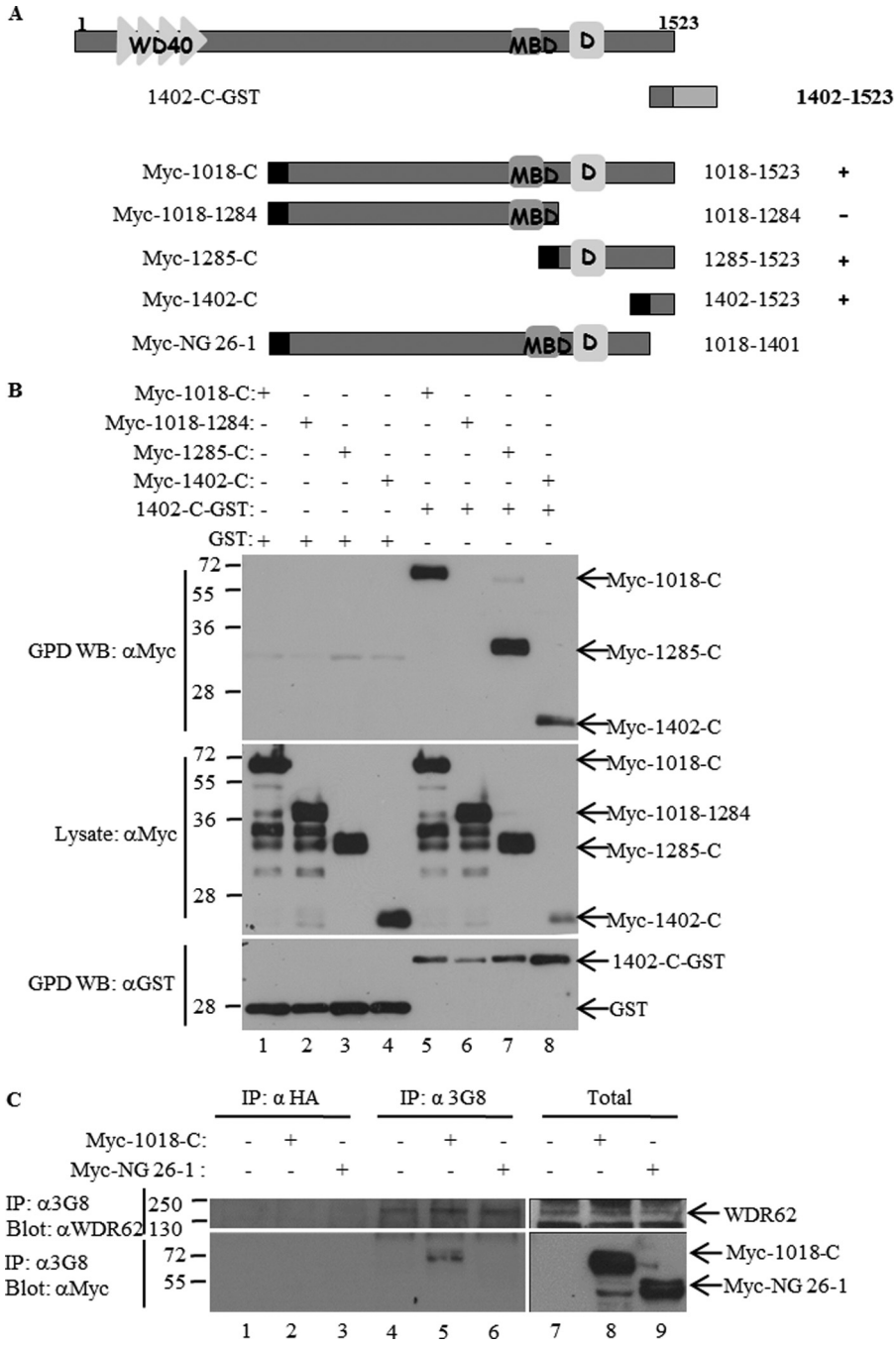

FIGURE 2. **The WDR62 C-terminal 122-amino acid fragment is sufficient for dimerization.** *A*, schematic represents WDR62 deletion constructs used in the experiments (as described in Fig. 1*A*). The construct indicated as NG 26-1 represents a premature termination codon mutation found in a microcephaly patient (12). *B*, HEK-293T cells were transfected with the indicated plasmids. GST-containing complexes were isolated from cell lysates with glutathione-agarose beads, washed extensively, and eluted with reduced glutathione (*GPD*) followed by Western blotting with either anti-Myc (*top panel*) or anti-GST (*bottom panel*) antibodies. The expression level of transfected WDR62 fragments was determined by blotting the total cell lysate with an anti-Myc antibody (*middle panel*). The migration of the relevant proteins is indicated by *arrows*. *C*, HEK-293T cells were transfected with either Myc-WDR62-1018-C or Myc-NG 26-1. Lysate was immunoprecipitated (*IP*) with either anti-3G8 antibody or anti-HA antibody (control) followed by Western blotting with either anti-Myc (*lower panel*) or anti-WDR62 antibodies (*upper panel*). The expression level of transfected WDR62 fragments and WDR62 endogenous protein was determined by blotting the total cell lysate with an anti-Myc antibody and an anti-WDR62 antibody (*right side*).

(Myc-NG 26-1-α3, Fig. 4*B*). Significantly, the loop-α3-helix structural motif was sufficient to dimerize with Myc-1018-C-GST fragment (Fig. 4*C*, *lane 6*). Consistently, WDR62 construct containing only the first two helices (NG 26-1-α1α2, supplemental Fig. 2*A*) failed to associate with HA-1402-C fragment (supplemental Fig. 2*B*, *lane 8*). Importantly, WDR62 dimerization formed via the loop-α3-helix was able to fully reconstitute the recruitment of either HA-JNK2 (Fig. 4*D*, *lane 4*) or GST-JNK2 (supplemental Fig. 3, *A* and *B*). In addition, the WDR62 fragment containing the loop-α3-helix was able to efficiently recruit GST-MKK7β1 (Fig. 4, *E* and *F*).

MAPKBP1 Homodimerization and Heterodimerization with WDR62—WDR62 dimerization domain shares a high degree of conservation with its putative orthologues (supplemental Fig.

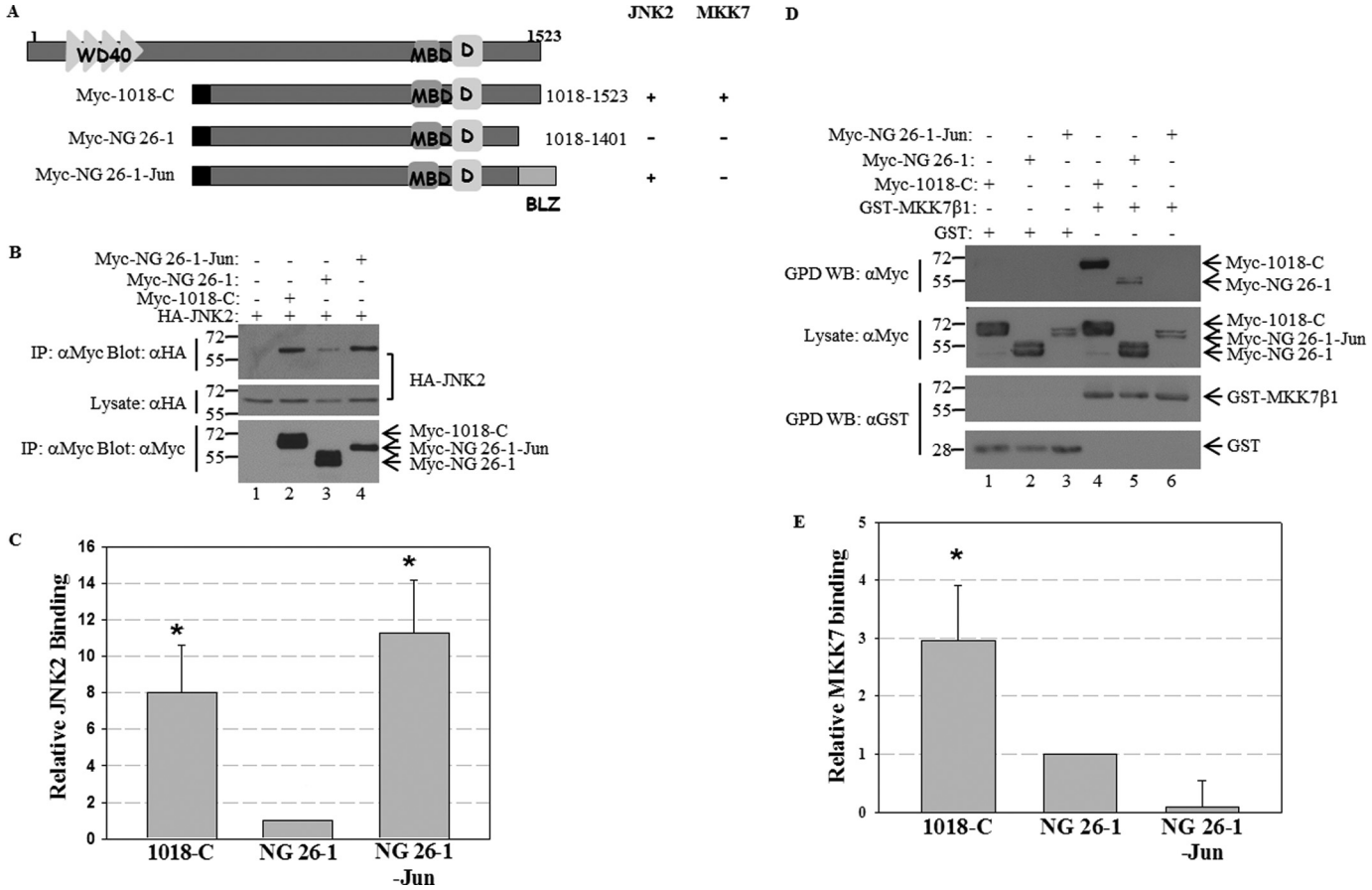

FIGURE 3. **WDR62 mutant with forced dimerization recapitulates JNK recruitment.** *A*, schematic representing WDR62 deletion constructs used in the experiments. The *black square* represents the position of the Myc epitope tag. The c-Jun basic leucine zipper domain is indicated by a *light gray rectangle*. A summary of the binding of the various WDR62 fragments to HA-JNK2 and GST-MKK7β1 is indicated by +/−. *B*, HEK-293T cells transfected with the indicated plasmids together with HA-JNK2. Cell lysates were subjected to immunoprecipitation (*IP*) with anti-Myc antibodies followed by Western blotting with either anti-HA (*top panel*) or anti-Myc (*bottom panel*) antibodies. The expression level of transfected HA-JNK2 was determined by blotting the total cell lysate with an anti-HA antibody (*middle panel*). The migration of the relevant proteins is indicated by *arrows*. *C*, quantification of HA-JNK2 binding. The levels of immunoprecipitated Myc-tagged WDR62 fragments and HA-JNK2 were quantified using image analysis software. The level of HA-JNK2 was normalized by dividing it by the level of Myc-tagged fragment in each reaction. The results represent the mean ± S.E. (*error bars*) of four independent experiments. The ratio represents the -fold of JNK binding relative to binding obtained with the Myc-NG 26-1 mutant, determined as 1. The *asterisk* (*) represents a *p* value <0.05. *D*, HEK-293T cells were transfected with the indicated plasmids. GST-containing complexes were isolated from cell lysates with glutathione-agarose beads, washed extensively, and eluted with reduced glutathione (*GPD*) followed by Western blotting with either anti-Myc (*top panel*) or anti-GST (*bottom panel*) antibodies. The expression level of transfected WDR62 fragments was determined by blotting the total cell lysate with an anti-Myc antibody (*middle panel*). The migration of the relevant proteins is indicated by *arrows*. *E*, quantification of Myc-WDR62 fragment binding. The levels of precipitated Myc-tagged WDR62 fragments and their total lysate were quantified using image analysis software. The levels of Myc-WDR62 fragments were normalized by dividing them by the level of total Myc-tagged fragment in the lysate for each reaction. The results represent the mean and S.E. of three independent experiments. The ratio represents the-fold of each Myc-tagged fragments binding relative to binding obtained with the Myc-NG 26-1 mutant, determined as 1. The *asterisk* (*) represents a *p* value <0.05.

4). In addition, we noticed a significant conservation with a second protein corresponding to JNKBP1/MAPKBP1 homologue protein (8, 32). The latter shares an overall 40% identity with WDR62 and a very high degree of identity along the last 20 amino acids (72%), which corresponds to the loop-helix 3 motif of WDR62 (supplemental Fig. 4, *bottom list*). Importantly, there is no information about the ability of MAPKBP1 to form dimers. Based on the high degree of homology with WDR62, we sought to examine the ability of MAPKBP1 to form dimers. We designed plasmids encoding for HA- and Myc-tagged MAPKBP1 corresponding to the last 200 amino acids (Fig. 5*A*). By using co-immunoprecipitation we have indeed shown that the MAPKBP1 C-terminal domain is able to form homodimers (Fig. 5*B*, *lane 3*). Moreover, because the WDR62 and MAPKBP1 dimerization domains are highly conserved, we examined their ability to form heterodimers with WDR62. Toward this end, we used the Myc-tagged C-terminal dimerization domain of MAPKBP1 and the 1018-C-GST construct of WDR62 (Fig. 5*A*). A GST pulldown strongly suggests that Myc-MAPKBP1-C efficiently associates with WDR62 to a similar extent as Myc-1018-C (Fig. 5*C*, compare *lane 3* with *lane 4*). Collectively, MAPKBP1 efficiently forms dimers and associates with WDR62 via the C-terminal loop-helix motif. To examine WDR62 and MAPKBP1 interaction in cells, HEK-293T cells were transfected with a Myc-MAPKBP1-C fragment followed by a 1-h treatment with arsenite (0.5 mM) prior to cell harvesting. Subsequently, the endogenous WDR62 protein was precipitated by the anti-3G8 monoclonal antibody (Fig. 5*D*). Indeed, WDR62 precipitation resulted in co-precipitation of the MAPKBP1 C-terminal fragment, demonstrating the possibility of the endogenous protein interaction. Next we studied WDR62 and MAPKBP1 co-localization using immunofluorescence

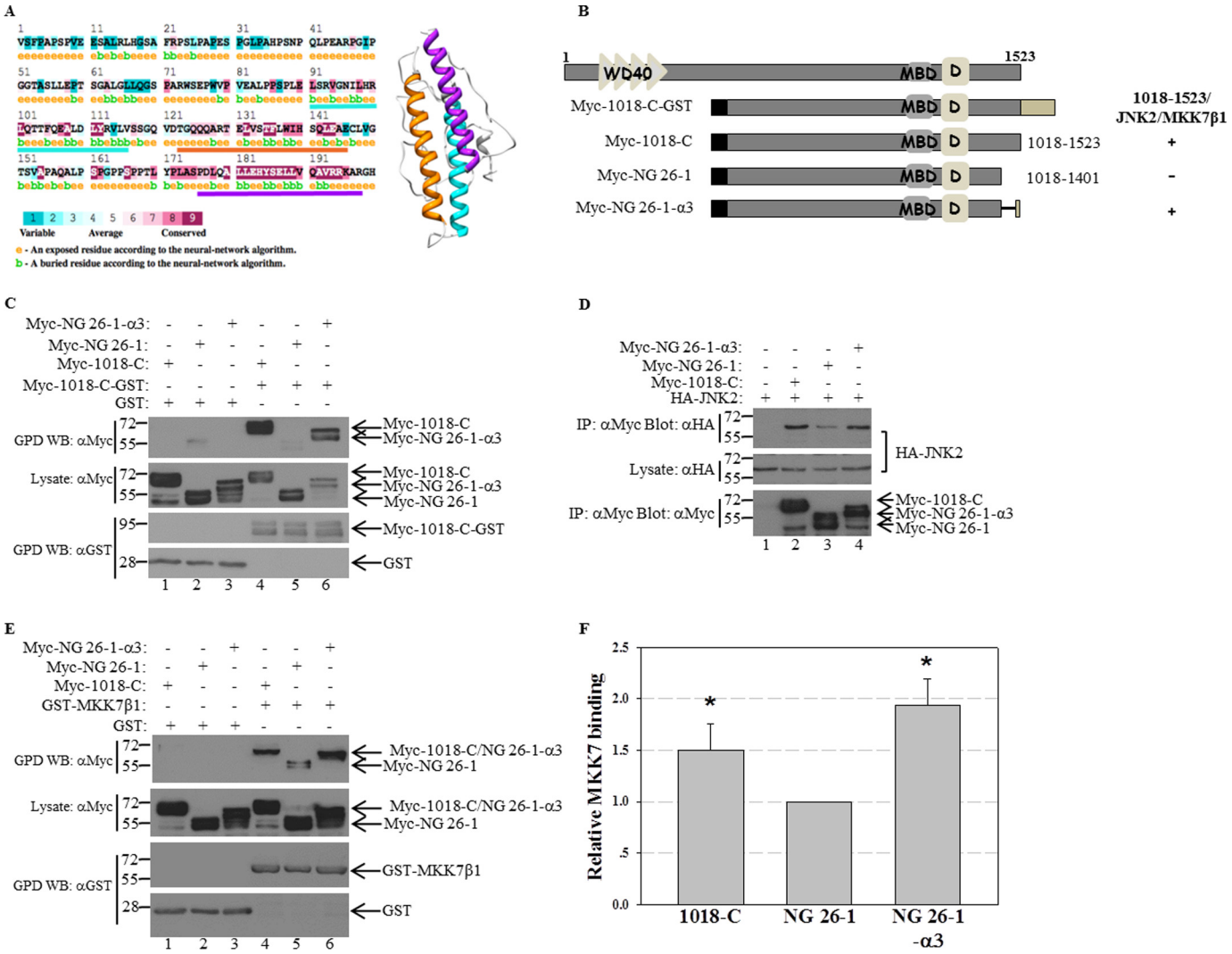

FIGURE 4. **Evolutionary conservation and secondary structure analysis of the C terminus reveals three putative α-helices, with the latter being the most conserved and necessary for WDR62 dimerization.** *A*, evolutionary conservation, secondary structure, and exposure prediction for the last 200 residues of WDR62 human based on 30-sequence SATe alignment. Evolutionary conservation scores were produced by the ConSurf server, color-coded: the *maroon-white-cyan* color scale (*i.e.* highly conserved-average-highly variable). Predicted buried (*b*) and exposed (*e*) residues are indicated below the protein sequence. The high conservation, the alternative buried and exposed residues (amphipathicity) and the secondary structure predictions strongly suggest the existence of three α-helices encompassing residues 91–116 (*cyan*), 123–146 (*orange*), and 176–198 (*purple*), indicated by a *thick colored line*. *Right panel*, one of the five modeled structures of the last 200 amino acids of human WDR62 obtained from the QUARK server, indicating the location of the predicted helices colored as on the *left panel*. *B*, schematic representation of the WDR62 deletion constructs used in the experiments. The *light gray rectangle* represents the position of the GST tag. The *black square* represents the position of the Myc epitope tag. Summary of the binding of the various WDR62 fragments to Myc-1018-C-GST is indicated by +/−. *C* and *E*, HEK-293T cells transfected with the indicated plasmids. GST-containing complexes were isolated from cell lysates with glutathione-agarose beads, washed extensively, and eluted with reduced glutathione (*GPD*) followed by Western blotting with either anti-Myc (*top panel*) or anti-GST (*bottom panel*) antibodies. The expression level of transfected WDR62 fragments was determined by blotting the total cell lysate with an anti-Myc antibody (*middle panel*). The migration of the relevant proteins is indicated by *arrows*. *D*, HEK-293T cells co-transfected with the indicated plasmids together with HA-JNK2. Cell lysates were subjected to immunoprecipitation (*IP*) with anti-Myc antibodies followed by Western blotting with either anti-HA (*top panel*) or anti-Myc (*bottom panel*) antibodies. The expression level of transfected HA-JNK2 was determined by blotting the total cell lysate with an anti-HA antibody (*middle panel*). The migration of the relevant proteins is indicated by *arrows*. *F*, quantification of Myc-WDR62 fragment binding. The levels of precipitated Myc-tagged WDR62 fragments and their total lysate were quantified using image analysis software. The levels of Myc-WDR62 fragments were normalized by dividing them by the level of total Myc-tagged fragment in the lysate for each reaction. The results represent the mean ± S.E. (*error bars*) of three independent experiments. The ratio represents the -fold of each Myc-tagged fragments binding relative to binding obtained with the Myc-NG 26-1 mutant, determined as 1. The *asterisk* (*) represents a *p* value <0.05.

analysis. First, HEK-293T cells transfected with Myc-MAPKBP1 expression plasmid were stained with anti-MAPKBP1 antibody to confirm the specificity of the purchased antibody used for immunofluorescence (supplemental Fig. 5). Importantly, WDR62 and MAPKBP1 antibodies displayed specific staining to their corresponding proteins with no apparent cross-reactivity (data not shown and Fig. 6*C*). Subsequently, HEK-293T exponentially growing cells were either left untreated or treated with arsenite for 1 h. Immunofluorescence analysis strongly suggests that the endogenous WDR62 protein and MAPKBP1 protein co-localize to stress granules following arsenite treatment (Fig. 6*A*). In addition, unlike WDR62, a partial co-localization was observed between MAPKBP1 and a processing bodies marker, DCP1A (Fig. 6*B*). Interestingly, no co-localization was observed in centrosomes in cells during mitosis (Fig. 6*C*). Therefore, we conclude that WDR62 and

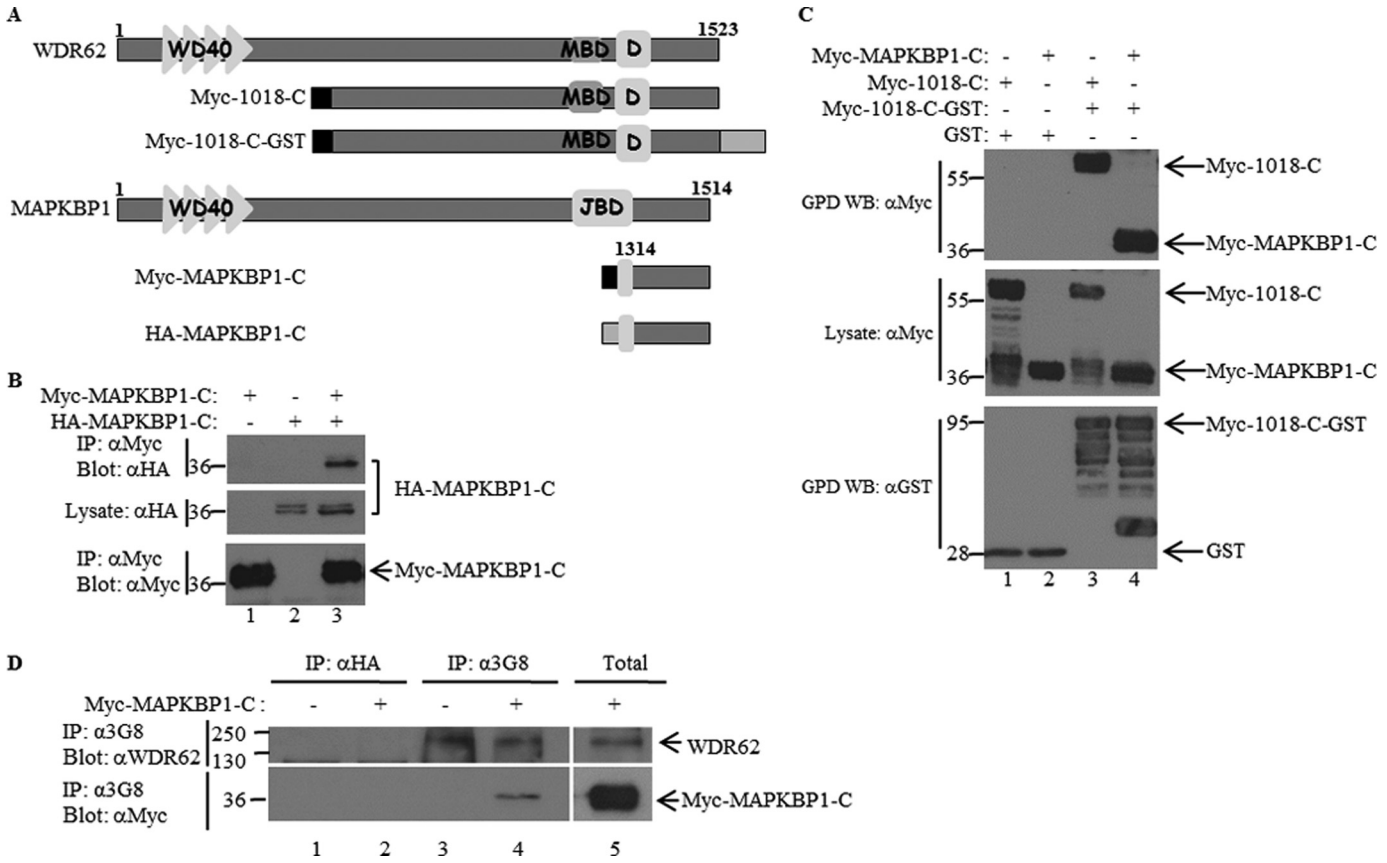

FIGURE 5. **MAPKBP1 is able to form homodimers as well as heterodimers with WDR62.** *A*, schematic representation of the WDR62 and MAPKBP1 deletion constructs used in the experiments. The *black square* or *light gray square* represents the position of the Myc epitope or HA epitope tags, respectively. The *light gray rectangle* represents the position of the GST tag. *B*, HEK-293T cells transfected with the indicated plasmids. Cell lysates were subjected to immunoprecipitation (*IP*) with anti-Myc antibodies followed by Western blotting with either anti-HA (*top panel*) or anti-Myc (*bottom panel*) antibodies. The expression level of transfected HA-MAPKBP1-C was determined by blotting the total cell lysate with an anti-HA antibody (*middle panel*). The migration of the relevant proteins is indicated by *arrows*. *C*, HEK-293T cells transfected with the indicated plasmids. GST-containing complexes were isolated from cell lysates with glutathione-agarose beads, washed extensively, and eluted with reduced glutathione (*GPD*), followed by Western blotting with either anti-Myc (*top panel*) or anti-GST (*bottom panel*) antibodies. The expression level of the transfected WDR62 and MAPKBP1 fragments was determined by blotting the total cell lysate with an anti-Myc antibody (*middle panel*). The migration of the relevant proteins is indicated by *arrows*. *D*, HEK-293T cells transfected with Myc-MAPKBP1-C. 24 h following transfection cells were treated with arsenite (0.5 mM) for 1 h. Lysate was immunoprecipitated with either anti-3G8 antibody or anti-HA antibody (control), followed by Western blotting with either anti-Myc (*lower panel*) or anti-WDR62 antibodies (*upper panel*). The expression level of transfected Myc-MAPKBP1-C fragment and WDR62 endogenous protein was determined by blotting the total cell lysate with an anti-Myc antibody and an anti-WDR62 antibody (*right side*). The migration of the relevant proteins is indicated by *arrows*.

MAPKBP1 interaction may occur *in vivo* through the C-terminal loop-α3-helix domain, and their interaction is being selectively regulated.

DISCUSSION

WDR62 is a novel JNK scaffold protein that specifically associates with MKK4/7 (MAP2K) and all three JNK isoforms (MAPK) (10, 11). The docking domains within WDR62 for MKK4/7 and JNKs are distinct, and the complex assembly occurs in an independent manner (11). WDR62 was found to be mutated in patients with microcephaly and severe brain malformations (12). While the multiple identified missense mutations are being scattered along the WDR62 protein, several premature translation terminations occur as well. The most striking of these is the premature termination codon that occurs at the C terminus of WDR62. A case in point is the NG 26-1 mutant which lacks the last 122 amino acids (12). Surprisingly, this C-terminal truncation does not preclude the WDR62 docking domains for either JNK or MKK4/7 and is therefore expected to associate with them. However, the patient phenotype is as severe as WDR62-null expression. Accordingly, we hypothesized that the C-terminal domain harbors a critical regulatory functional role. Here, we mapped the WDR62 dimerization domain to the C-terminal region. The sequence responsible for WDR62 dimerization has no apparent homology to a known oligomerization domain. This domain was found to be both necessary and sufficient for WDR62 homodimerization. Fusion of a functional bZIP dimerization motif from c-Jun to the WDR62 mutant that lacked the dimerization domain was sufficient to recapitulate the recruitment of JNK2; however, it was not enough for MKK7β1-efficient association. Using bioinformatics, we were able to identify a loop-α3-helix motif. Interestingly, we demonstrated that WDR62 dimerization via the third α-helix significantly facilitates the association with MKK7β1 and JNK2. Whereas JNK does not require dimerization for its activity, WDR62 dimerization most likely serves to increase the avidity to JNK and to facilitate its recruitment. This is especially so in view of the fact that the JNK docking domain identified within WDR62 displays a reduced IC_{50} compared

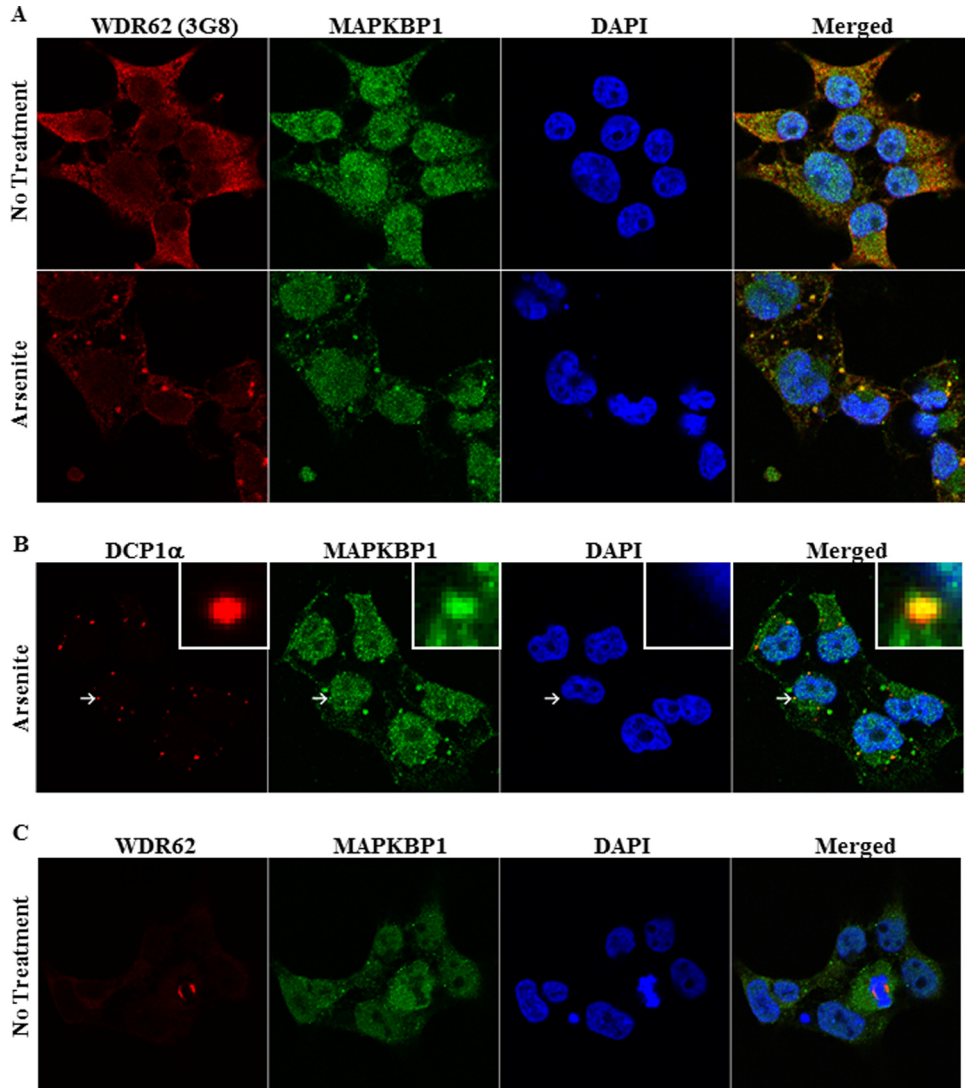

FIGURE 6. **MAPKBP1 co-localizes with WDR62 in stress granules but not in centrosomes.** *A*, immunofluorescence of HEK-293T cells that are either untreated or treated with arsenite. Fixed cells were stained for WDR62 (3G8, *red*), MAPKBP1 (*green*), and DAPI nuclear stain (*blue*). *B*, immunofluorescence of HEK-293T cells either untreated or treated with arsenite. Fixed cells were stained for DCP1A (*red*), MAPKBP1 (*green*), and DAPI nuclear stain (*blue*). Representative processing body with co-localization of MAPKBP1 is *highlighted* by an *arrow* in the image and shown enlarged in *insets*. *C*, immunofluorescence of HEK-293T cells during mitosis stained as described in *A*.

with JIP peptide (10). On the other hand, the fact that MKK7β1 could not be recruited to WDR62 forced-dimer and could only be recruited to WDR62 dimerization through its last α-helix suggests that MKK7β1 binding to WDR62 requires additional signals beside dimerization, which are yet to be identified.

Multiple protein kinases are activated following dimerization. For example, growth factor tyrosine kinase receptors can be activated by aggregating their extracellular ligand binding domains by their corresponding ligands (33). Similarly, the nonreceptor lymphocyte-specific protein tyrosine kinase (LCK) forms dimers following its activation through a typical SH3-polyproline-rich region interaction (34). In addition, B-Raf (35), dual leucine zipper-bearing kinase (DLK) and members of the mixed lineage kinase (MLK) family require dimerization for their subsequent activation (36). Interestingly, several scaffold proteins were shown to form dimers (9, 29, 37). One of the first studied scaffold proteins found in *Saccharomyces cerevisiae* is Ste5 which was found to dimerize through an N-terminal dimerization domain. Ste5 dimerization correlates with its ability to regulate the pheromone MAPK signaling pathway (38).

The WDR62 functional homologues JIP 1–3 were also shown to homo- and heterodimerize via an atypical SH3-SH3 interaction motif (39–41). JIP dimerization serves to regulate association with DLK (MAP3K. JIP-DLK association renders DLK in a monomeric inactive form. DLK-JIP complex dissociates after JIP phosphorylation allowing DLK subsequent dimerization and activation (20, 36). JIP mutations that impair its dimerization ability do not weaken JIP binding to JNK, MKK7, or MLK3 (41). In contrast, the WDR62 mutant lacking the dimerization domain in the present study failed to associate with JNK2 and MKK7β1 thereby abrogating the WDR62 scaffolding function of the JNK signaling pathway. JIP proteins were also shown to associate with the distant JNK scaffold protein, POSH (42). POSH-JIP association is required to mediate MLK3 association with the JNK modules that are responsible for activation of the

apoptotic pathway (42). Interestingly, dimer-specific JIP antibodies identified phosphorylated JIP dimers in the nucleus, whereas unphosphorylated JIP monomers reside in the cytoplasm (43). Whereas the WDR62 wild-type protein is confined to cellular granules, the NG 26-1 mutant is dispersed in the cytoplasm. Whether the WDR62 localization to the cellular granules is dependent on WDR62 dimerization or complex assembly waits to be studied.

Using a combination of bioinformatics prediction analysis with biochemical support, we were able to provide evidence for the possible existence of three putative α-helices structural motif within the dimerization domain. Subsequently, this analysis further facilitated a fine mapping of the sequence-structural requirements for WDR62 dimerization motif to the third loop-helix motif.

This loop-helix motif is composed of an N-terminal highly flexible subdomain that is rich in proline, serine, and glycine residues (with three conserved pairs of SP), followed by a C-terminal α-helix composed of a highly conserved charged residues intercalated with hydrophobic residues (supplemental Fig. 6).

Interestingly, the loop-helix domain displays a high degree of sequence homology with WDR62 orthologues and a second related protein MAPKBP1. We also obtained evidence that the MAPKBP1-conserved C-terminal domain is able to form dimers and heterodimers with WDR62 fragment and endogenous protein. Prior to the present study, the association between WDR62 and MAPKBP1 could not be predicted based on the available knowledge. WDR62 and MAPKBP1 are co-localized in stress granules following stress, which means that the interaction is potentially possible, whereas no apparent co-localization and interaction occur during mitosis. The precise mechanism that regulates the interaction between the distinct JNK scaffold proteins is yet to be determined.

The interaction between distinct scaffold proteins greatly enhances the potential regulatory complexity within the same signaling tier. This situation may provide a mechanism which allows cross-talk between scaffold proteins of other signaling tiers. Therefore, the present study suggests another layer of complexity in signal transduction, resulting in a possible coordinated activation of multiple signaling pathways via the association between scaffold proteins.

Acknowledgments—We thank Aviva Cohen for technical assistance and Drs. Katsuji Yoshioka (Kanazawa, Japan) and Michihiko Ito (Kanagawa, Japan) for the Myc-MAPKBP1 expression plasmid.

REFERENCES

1. Dhanasekaran, D. N., and Johnson, G. L. (2007) MAPKs: function, regulation, role in cancer and therapeutic targeting. *Oncogene* **26,** 3097–3099
2. Good, M. C., Zalatan, J. G., and Lim, W. A. (2011) Scaffold proteins: hubs for controlling the flow of cellular information. *Science* **332,** 680–686
3. Enslen, H., and Davis, R. J. (2001) Regulation of MAP kinases by docking domains. *Biol. Cell* **93,** 5–14
4. Johnson, G. L., and Nakamura, K. (2007) The c-Jun kinase/stress-activated pathway: regulation, function and role in human disease. *Biochim. Biophys. Acta* **1773,** 1341–1348
5. Haeusgen, W., Herdegen, T., and Waetzig, V. (2011) The bottleneck of JNK signaling: molecular and functional characteristics of MKK4 and MKK7. *Eur. J. Cell Biol.* **90,** 536–544
6. Weston, C. R., Lambright, D. G., and Davis, R. J. (2002) MAP kinase signaling specificity. *Science* **296,** 2345–2347
7. Holmberg, C., Katz, S., Lerdrup, M., Herdegen, T., Jäättelä, M., Aronheim, A., and Kallunki, T. (2002) A novel specific role for IκB kinase complex-associated protein in cytosolic stress signaling. *J. Biol. Chem.* **277,** 31918–31928
8. Koyano, S., Ito, M., Takamatsu, N., Shiba, T., Yamamoto, K., and Yoshioka, K. (1999) A novel Jun N-terminal kinase (JNK)-binding protein that enhances the activation of JNK by MEK kinase 1 and TGF-β-activated kinase 1. *FEBS Lett.* **457,** 385–388
9. Dhanasekaran, D. N., Kashef, K., Lee, C. M., Xu, H., and Reddy, E. P. (2007) Scaffold proteins of MAP-kinase modules. *Oncogene* **26,** 3185–3202
10. Wasserman, T., Katsenelson, K., Daniliuc, S., Hasin, T., Choder, M., and Aronheim, A. (2010) A novel c-Jun N-terminal kinase (JNK)-binding protein WDR62 is recruited to stress granules and mediates a nonclassical JNK activation. *Mol. Biol. Cell* **21,** 117–130
11. Cohen-Katsenelson, K., Wasserman, T., Khateb, S., Whitmarsh, A. J., and Aronheim, A. (2011) Docking interactions of the JNK scaffold protein WDR62. *Biochem. J.* **439,** 381–390
12. Bilgüvar, K., Oztürk, A. K., Louvi, A., Kwan, K. Y., Choi, M., Tatli, B., Yalnizoğlu, D., Tüysüz, B., Cağlayan, A. O., Gökben, S., Kaymakçalan, H., Barak, T., Bakircioğlu, M., Yasuno, K., Ho, W., Sanders, S., Zhu, Y., Yilmaz, S., Dinçer, A., Johnson, M. H., Bronen, R. A., Koçer, N., Per, H., Mane, S., Pamir, M. N., Yalçinkaya, C., Kumandaş, S., Topçu, M., Ozmen, M., Sestan, N., Lifton, R. P., State, M. W., and Günel, M. (2010) Whole-exome sequencing identifies recessive WDR62 mutations in severe brain malformations. *Nature* **467,** 207–210
13. Yu, T. W., Mochida, G. H., Tischfield, D. J., Sgaier, S. K., Flores-Sarnat, L., Sergi, C. M., Topçu, M., McDonald, M. T., Barry, B. J., Felie, J. M., Sunu, C., Dobyns, W. B., Folkerth, R. D., Barkovich, A. J., and Walsh, C. A. (2010) Mutations in WDR62, encoding a centrosome-associated protein, cause microcephaly with simplified gyri and abnormal cortical architecture. *Nat. Genet.* **42,** 1015–1020
14. Nicholas, A. K., Khurshid, M., Désir, J., Carvalho, O. P., Cox, J. J., Thornton, G., Kausar, R., Ansar, M., Ahmad, W., Verloes, A., Passemard, S., Misson, J. P., Lindsay, S., Gergely, F., Dobyns, W. B., Roberts, E., Abramowicz, M., and Woods, C. G. (2010) WDR62 is associated with the spindle pole and is mutated in human microcephaly. *Nat. Genet.* **42,** 1010–1014
15. Bhat, V., Girimaji, S. C., Mohan, G., Arvinda, H. R., Singhmar, P., Duvvari, M. R., and Kumar, A. (2011) Mutations in WDR62, encoding a centrosomal and nuclear protein, in Indian primary microcephaly families with cortical malformations. *Clin. Genet.* **80,** 532–540
16. Kousar, R., Hassan, M. J., Khan, B., Basit, S., Mahmood, S., Mir, A., Ahmad, W., and Ansar, M. (2011) Mutations in WDR62 gene in Pakistani families with autosomal recessive primary microcephaly. *BMC Neurol.* **11,** 119
17. Zaki, M. S., Salam, G. M., Saleem, S. N., Dobyns, W. B., Issa, M. Y., Sattar, S., and Gleeson, J. G. (2011) New recessive syndrome of microcephaly, cerebellar hypoplasia, and congenital heart conduction defect. *Am. J. Med. Genet. A* **155A,** 3035–3041
18. Biesecker, L. G. (2011) Editorial comment on "Whole exome sequencing identifies compound heterozygous mutations in WDR62 in siblings with recurrent polymicrogyria." *Am. J. Med. Genet. A.* **155A,** 2069–2070
19. Bogoyevitch, M. A., Yeap, Y. Y., Qu, Z., Ngoei, K. R., Yip, Y. Y., Zhao, T. T., Heng, J. I., and Ng, D. C. (2012) WD40-repeat protein 62 is a JNK-phosphorylated spindle pole protein required for spindle maintenance and timely mitotic progression. *J. Cell Sci.* **125,** 5096–5109
20. Mooney, L. M., and Whitmarsh, A. J. (2004) Docking interactions in the c-Jun N-terminal kinase pathway. *J. Biol. Chem.* **279,** 11843–11852
21. Dimmer, E. C., Huntley, R. P., Alam-Faruque, Y., Sawford, T., O'Donovan, C., Martin, M. J., Bely, B., Browne, P., Mun Chan, W., Eberhardt, R., Gardner, M., Laiho, K., Legge, D., Magrane, M., Pichler, K., Poggioli, D., Sehra, H., Auchincloss, A., Axelsen, K., Blatter, M. C., Boutet, E., Braconi-Quintaje, S., Breuza, L., Bridge, A., Coudert, E., Estreicher, A., Famiglietti, L., Ferro-Rojas, S., Feuermann, M., Gos, A., Gruaz-Gumowski, N., Hinz, U., Hulo, C., James, J., Jimenez, S., Jungo, F., Keller, G., Lemercier, P., Lieberherr, D., Masson, P., Moinat, M., Pedruzzi, I., Poux, S., Rivoire, C., Roechert, B., Schneider, M., Stutz, A., Sundaram, S., Tognolli, M., Bougueleret, L., Argoud-Puy, G., Cusin, I., Duek-Roggli, P., Xenarios, I., and

Apweiler, R. (2012) The UniProt-GO Annotation database in 2011. *Nucleic Acids Res.* **40,** D565–570
22. Löytynoja, A., and Goldman, N. (2005) An algorithm for progressive multiple alignment of sequences with insertions. *Proc. Natl. Acad. Sci. U.S.A.* **102,** 10557–10562
23. Finn, R. D., Clements, J., and Eddy, S. R. (2011) HMMER web server: interactive sequence similarity searching. *Nucleic Acids Res.* **39,** W29–37
24. Liu, K., Warnow, T. J., Holder, M. T., Nelesen, S. M., Yu, J., Stamatakis, A. P., and Linder, C. R. (2012) SATe-II: very fast and accurate simultaneous estimation of multiple sequence alignments and phylogenetic trees. *Syst. Biol.* **61,** 90–106
25. Berezin, C., Glaser, F., Rosenberg, J., Paz, I., Pupko, T., Fariselli, P., Casadio, R., and Ben-Tal, N. (2004) ConSeq: the identification of functionally and structurally important residues in protein sequences. *Bioinformatics* **20,** 1322–1324
26. Ashkenazy, H., Erez, E., Martz, E., Pupko, T., and Ben-Tal, N. (2010) ConSurf 2010: calculating evolutionary conservation in sequence and structure of proteins and nucleic acids. *Nucleic Acids Res.* **38,** W529–533
27. Kurowski, M. A., and Bujnicki, J. M. (2003) GeneSilico protein structure prediction meta-server. *Nucleic Acids Res.* **31,** 3305–3307
28. Crooks, G. E., Hon, G., Chandonia, J. M., and Brenner, S. E. (2004) WebLogo: a sequence logo generator. *Genome Res.* **14,** 1188–1190
29. Whitmarsh, A. J. (2006) The JIP family of MAPK scaffold proteins. *Biochem. Soc. Trans.* **34,** 828–832
30. Aronheim, A., Zandi, E., Hennemann, H., Elledge, S. J., and Karin, M. (1997) Isolation of an AP-1 repressor by a novel method for detecting protein-protein interactions. *Mol. Cell. Biol.* **17,** 3094–3102
31. Weidenfeld-Baranboim, K., Bitton-Worms, K., and Aronheim, A. (2008) TRE-dependent transcription activation by JDP2-CHOP10 association. *Nucleic Acids Res.* **36,** 3608–3619
32. Yamaguchi, T., Miyashita, C., Koyano, S., Kanda, H., Yoshioka, K., Shiba, T., Takamatsu, N., and Ito, M. (2009) JNK-binding protein 1 regulates NF-κB activation through TRAF2 and TAK1. *Cell Biol. Int.* **33,** 364–368
33. Alroy, I., and Yarden, Y. (1997) The ErbB signaling network in embryogenesis and oncogenesis: signal diversification through combinatorial ligand-receptor interactions. *FEBS Lett.* **410,** 83–86
34. Eck, M. J., Atwell, S. K., Shoelson, S. E., and Harrison, S. C. (1994) Structure of the regulatory domains of the Src-family tyrosine kinase Lck. *Nature* **368,** 764–769
35. Rajakulendran, T., Sahmi, M., Lefrançois, M., Sicheri, F., and Therrien, M. (2009) A dimerization-dependent mechanism drives RAF catalytic activation. *Nature* **461,** 542–545
36. Nihalani, D., Meyer, D., Pajni, S., and Holzman, L. B. (2001) Mixed lineage kinase-dependent JNK activation is governed by interactions of scaffold protein JIP with MAPK module components. *EMBO J.* **20,** 3447–3458
37. Dard, N., and Peter, M. (2006) Scaffold proteins in MAP kinase signaling: more than simple passive activating platforms. *Bioessays* **28,** 146–156
38. Yablonski, D., Marbach, I., and Levitzki, A. (1996) Dimerization of Ste5, a mitogen-activated protein kinase cascade scaffold protein, is required for signal transduction. *Proc. Natl. Acad. Sci. U.S.A.* **93,** 13864–13869
39. Yasuda, J., Whitmarsh, A. J., Cavanagh, J., Sharma, M., and Davis, R. J. (1999) The JIP group of mitogen-activated protein kinase scaffold proteins. *Mol. Cell. Biol.* **19,** 7245–7254
40. Kelkar, N., Gupta, S., Dickens, M., and Davis, R. J. (2000) Interaction of a mitogen-activated protein kinase signaling module with the neuronal protein JIP3. *Mol. Cell. Biol.* **20,** 1030–1043
41. Kristensen, O., Guenat, S., Dar, I., Allaman-Pillet, N., Abderrahmani, A., Ferdaoussi, M., Roduit, R., Maurer, F., Beckmann, J. S., Kastrup, J. S., Gajhede, M., and Bonny, C. (2006) A unique set of SH3-SH3 interactions controls IB1 homodimerization. *EMBO J.* **25,** 785–797
42. Kukekov, N. V., Xu, Z., and Greene, L. A. (2006) Direct interaction of the molecular scaffolds POSH and JIP is required for apoptotic activation of JNKs. *J. Biol. Chem.* **281,** 15517–15524
43. Borsello, T., Centeno, C., Riederer, I. M., Haefliger, J. A., and Riederer, B. M. (2007) Phosphorylation-dependent dimerization and subcellular localization of islet-brain 1/c-Jun N-terminal kinase-interacting protein 1. *J. Neurosci. Res.* **85,** 3632–3641